Bull Volcanol (2010) 72:411–429
DOI 10.1007/s00445-009-0334-2

RESEARCH ARTICLE

# Hazard and risk assessment in a complex multi-source volcanic area: the example of the Campania Region, Italy

**L. Lirer · P. Petrosino · I. Alberico**

Received: 14 April 2008 / Accepted: 1 December 2009 / Published online: 19 January 2010


**Abstract** In order to zone the territory of Campania Region (southern Italy) with regard to the hazard related to future explosive activity of Somma-Vesuvio, Campi Flegrei, and Ischia Island, we drew a multi-source hazard map for tephra and pyroclastic flows. This map, which merges the areas possibly endangered by the three volcanic sources, takes into account a large set of tephra fall and pyroclastic flow events that have occurred in the last 10 ka. In detail, for fall products at Campi Flegrei and Somma-Vesuvio we used the dispersal of past eruption products as deduced by field surveys and their recurrence over the whole area. For pyroclastic flows, the field data were integrated with VEI=4 simulated events; about 100 simulations sourcing from different points of the area were performed, considering the different probability of vent opening. The spatial recurrence of products of both past eruptions and simulated events was used to assign a weight to the area endangered by the single volcanic sources. The sum of these weights in the areas exposed to the activity of two sources and/or to different kinds of products was used to draw a hazard map, which highlights the spatial trend and the extent of the single equivalent classes at a regional scale. A multi-source risk map was developed for the same areas as the graphic result of the product of volcanic hazard and exposure, assessed in detail from a dasymetric map. The resulting multi-source hazard and risk maps are essential tools for communication among scientists, local authorities, and the public, and may prove highly practical for long-term regional-scale mitigation planning.

**Keywords** Somma-Vesuvio · Campi Flegrei · Ischia Island · Volcanic hazard · Volcanic risk · Campania Region

Editorial responsibility R. Cioni

L. Lirer · P. Petrosino (✉)
Dipartimento di Scienze della Terra,
Università degli Studi di Napoli "Federico II",
Largo S. Marcellino 10,
Napoli, Italy
e-mail: petrosin@unina.it

L. Lirer
e-mail: lirer@unina.it

I. Alberico
Centro Interdipartimentale Ricerca Ambiente (CIRAM),
Università degli Studi di Napoli "Federico II",
Via Mezzocannone 16,
Napoli, Italy
e-mail: ialberic@unina.it

## Introduction

Somma-Vesuvio, Campi Flegrei, and Ischia Island are three active volcanic sources endangering much of the Campania Region (southern Italy). These volcanoes are universally known for their high risk due to the probability of occurrence of a new explosive eruption in a densely populated area, where about 3.5 million people live.

The assessment of volcanic hazard and analysis of the socio-politico-economical context are necessary both for the short-term to manage volcanic crises, and for the long-term to reduce volcanic risk. The risk formula (Risk = Hazard × Exposure × Vulnerability; UNDRO 1979) defines hazard as the probability of occurrence of a specified natural hazard at a specified severity level in a specified future time period, exposure as an inventory of those people or artefacts that are exposed to the hazard, and vulnerability as the degree of loss to each element should a hazardous event of a given severity occur (Coburn et al. 1991). Hence there is a need to define in detail not only the volcanic hazard and exposure but also the vulnerability.

Vulnerability is a complex parameter that depends on the features of the territory that influences its resistance to the impact, and its capacity to cope with the hazardous event. It includes *physical vulnerability* of exposed elements, depending on the resistance of buildings or infrastructure to the impact; *social vulnerability*, depending on the capacity of different groups to react to the event; *functional vulnerability*, depending on the effectiveness of warning procedures and emergency preparedness; and *systemic vulnerability*, depending on the mutual influences among the system elements. Unfortunately, at present no vulnerability assessment for volcanic activity for the entire multi-source Campania area is available, apart from some very recent papers detailing building vulnerability in the area near Vesuvio (Baxter et al. 2008; Zuccaro et al. 2008).

Despite the high hazard posed by volcanic sources, the population in Campania has increased remarkably in the last 40 years (Petrosino et al. 2004), thus contributing to a rise in volcanic risk. At Somma-Vesuvio, from 1961 to 1981, the population increased by 50% in coastal areas and 25% in the interior. At Campi Flegrei, between 1961 and 1971, the population increased by about 20%, and this increase reached 80% during the following decade. At both volcanic areas, the total population slightly decreased between 1981 and 2001 only because the territory became saturated (Petrosino et al. 2004). On the island of Ischia, the third active volcanic source of the Campania Region, over the last 40 years, the residential population has increased from 34,000 up to 56,000 people, with a mean decadal increment of about 20%. On the island, the population increases significantly in the summer due to the presence of tourists, increasing the number of people possibly endangered by a volcanic event.

The Regione Campania Authority has recently developed a plan aimed at reducing exposure at Somma-Vesuvio. It states that no new construction can be built in the perivolcanic area and encourages new families to settle elsewhere, in new urban developed areas outside the high hazard zone. At Campi Flegrei and Ischia Island, there are currently no governmental or regional authority plans or strategies aimed at reducing population in areas exposed to volcanic hazard.

The main purpose of the present paper is therefore to produce multi-source regional-scaled volcanic hazard and risk maps of Campania for tephra and pyroclastic flows (hereafter concisely defined multi-source hazard and risk maps) for an area exposed to hazard from the three different volcanic sources.

The most difficult task was finding a methodology that combined both hazard and risk assessment at a central volcano (Somma-Vesuvio) and at volcanic fields (Campi Flegrei and Ischia Island). For this, a detailed investigation of the eruptive events in the last 10 ka at the three volcanic sources was carried out. At Somma-Vesuvio, the dispersal of pyroclastic fall and flow products is very well depicted through field data (Andronico and Cioni 2002; Cioni et al. 1999; Lirer et al. 1993, 2001a; Rolandi et al. 1993a, 1993b, 1993c, 1998, 2004; Rosi et al. 1993; Santacroce et al. 2003). It was therefore possible to use the distribution data to draw the volcanic hazard map by taking into account the frequency of events and their magnitude.

The distribution of past products is much more complicated to use for hazard assessment at Campi Flegrei and Ischia Island. The absence of a spatial trend in the past monogenetic vent location, in fact, makes the source of a possible future eruption unpredictable. Because of this, field data were integrated with events simulated over the entire volcanic field. As far as the type and size of eruption is concerned, we simulated VEI (volcanic explosive index) = 4 explosive events producing pyroclastic flows, considering the typical magnitude of the largest Holocene events (Orsi et al. 2004; Brown et al. 2008). Finally, the distributions of the fall products of the high VEI eruptions at Campi Flegrei were processed by a procedure analogous to that used for Somma-Vesuvio.

In the end, a new quantification of exposure in terms of residential population density index, based on a statistical analysis, was performed to produce a detailed risk map.

The multi-source hazard and risk maps for tephra and pyroclastic flows here obtained are a very innovative tool because they allow people for the first time to gain a synoptic view of the areas possibly endangered by all the Campania volcanic sources. In as much, they show the spatial trend and the extent of the single hazard and risk class at regional scale and highlight the different risks characterizing adjacent areas (e.g., the northern and southern slope of Somma-Vesuvio).

## Volcanic hazard at the Campanian active volcanoes: state of knowledge

Spatial extent and different location of the areas possibly endangered by Somma-Vesuvio, Campi Flegrei, and Ischia Island are controlled by the contrasting nature of the volcanic sources, the type and magnitude of explosive eruptions, and the topography.

The undoubtedly different volumes of magma involved in the three areas are related to the different feeding systems. At Somma-Vesuvio, a central volcano, in fact, magma stagnates and differentiates in a deep complex magmatic reservoir, the top of which is about 8 km deep. Magmas rise from this reservoir to shallow magma chambers and feed the different eruptions with several cubic kilometers of magma (Civetta et al. 2004; Di Renzo et al. 2007) after variably long resting periods. In a very recent paper, Scaillet et al. (2008) used experimental phase equilibria to indicate that between 18.5 ka and 1944, the magma reservoir of Somma-Vesuvio migrated 9 to 11 km upward. Moreover, in relation to the products of the last two low-VEI explosive eruptions (1631 and 1944), they identified the occurrence of leucite and clinopyroxene crystals formed at <3 km depth, and proposed a model in which deep magma batches, coming from a deeper reservoir or directly from the source region, feed shallow reservoirs, where they reside 9 years or less before being erupted. Magma that fed the last recorded high magnitude eruption (Neapolitan Yellow Tuff, 15 ka, Deino et al. 2004) rested in a large and deep reservoir at Campi Flegrei volcanic field (D'Antonio et al. 1999). The monogenetic activity occurred after the Neapolitan Yellow Tuff eruption was fed in scattered points of the area by many small, shallower, independent magma pockets involving less than 1 $km^3$ of magma (D'Antonio 2005). Finally, at Ischia Island the presence of a deep magma reservoir, similar to that which fed the highly explosive Monte Epomeo eruption (55 ka, Poli et al. 1987), can be excluded (Brown et al. 2008). The eruptions of the last 5 ka were fed by dykes tapping small (less than 0.5 $km^3$) and shallow magma batches (Piochi et al. 1999).

The distribution of hazard areas strictly depends on the different eruptive typologies. Volcanic hazard maps for explosive events must take into account the size of the expected event and the kind of eruptive mechanism occurring during the eruption. The area of emplacement of a pyroclastic fall deposit, in fact, depends on the height of the column as well as on the atmospheric conditions (mainly wind direction and strength), and is not sensitive to the pre-existing topography. The probability of an area to be invaded by a pyroclastic flow is strictly related to the VEI of the event, the distance from the vent, and the morphology of the area proximal to the vent. At a volume discharge rate ranging between $10^3 m^3/s$ and $10^4 m^3/s$, as is typical of the explosive events that have occurred at Campi Flegrei and Ischia Island in the last 10 ka, the control of morphology on the travel distance will be predominant. At Campi Flegrei, the presence of scattered monogenetic edifices, with an average height of 200 m, results in a complex distribution of topographic obstacles, which can exert an important control over the pyroclastic flows emplacement (Lirer et al. 2001b). At Ischia Island, on the contrary, Monte Epomeo is a huge topographic barrier located in the center of the island, which could influence the pyroclastic flows' distribution, mainly in case of a future event sourcing in the coastal plains (Alberico et al. 2008).

Previous attempts of assessing hazard and risk deal with the single sources, one at a time, and overlook the fact that the Campania volcanoes make up a complex multi-source area and that several zones can be endangered by the products of more than one source.

A brief summary of previous studies dealing with hazard assessment at Somma-Vesuvio, Campi Flegrei, and Ischia Island is reported below and shown in Table 1. More in detail, the fundamentals and main parameters of the papers providing simulations of explosive eruptions are summarized in Table 2.

The analysis of the most recent (last 4,000 years) eruptive history of Somma-Vesuvio reveals the recurrence of highly explosive events followed by variably long periods during which low VEI strombolian and/or vulcanian events took place (Rolandi et al. 1998; Arrighi et al. 2001; Lirer et al. 2001a; Andronico and Cioni 2002; Cioni et al. 2003). Assuming that the past is a reasonable guide to the future behavior of the volcano, Lirer et al. (2001a) and Cioni et al. (2003) drew a spatial frequency hazard map for pyroclastic fall products by taking into account the whole set of sizes of past eruptions and related deposits. Moreover, Cioni et al. (2003) simulated theoretical sub-Plinian events using wind fields sampled between 1962 and 1976 at the Aeronautica Militare meteorological station of Brindisi and conclude that the volcanic hazard map drawn through the distributions of past products is more reliable in proximal areas, whereas the simulated events can furnish additional data for hazard assessment in distal areas. As a matter of fact, passing to Plinian events, a slight difference emerges in the hazard degree of the E–SE sector of the volcano, for which recent results based on the simulations of fall dispersal from 30–35 km high eruptive columns with a large sample of acting wind fields (Macedonio et al. 2008; Daniele et al. 2009) postulate a higher hazard degree.

Regarding pyroclastic flow hazard at Somma-Vesuvio, Lirer et al. (2001a) drew a spatial frequency map considering at risk the areas where the pyroclastic flows of the main explosive events of the last 4.0 ka were emplaced. Esposti Ongaro et al. (2002) simulated different pyroclastic flows by assuming different magmatic compositions, eruption intensities, topographic profiles, and flow durations. Their results emphasize the high hazard level of the perivolcanic area, extending to 8 km from the vent.

The behavior of the Campi Flegrei volcanic system after the Neapolitan Yellow Tuff eruption led Orsi et al. (2004) to infer that in case of renewal of volcanism in the short to middle term, the most probable event is an eruption of medium magnitude (VEI=4).

In this area, Petrosino et al. (2004) evaluated the pyroclastic fall hazard using a methodology similar to that previously applied by Lirer et al. (2001a) to Somma-Vesuvio. They took into account the distribution of the products of the two main eruptions of the last 10 ka, which hit most of the territory inside the Campi Flegrei caldera and

**Table 1** Summary of previous studies dealing with hazard assessment at Somma-Vesuvio, Campi Flegrei, and Ischia Island

| Paper | Source | Age range | Kind of products | Reported explosive eruptions | Field data | Simulations |
|---|---|---|---|---|---|---|
| Barberi et al. (1990) | Somma-Vesuvio | | Pyroclastic fall | | - | Yes |
| Lirer et al. (2001a) | Somma-Vesuvio | <10 ka | Pyroclastic fall and pyroclastic flow | 10 explosive events (3<VEI<5) emplacing pyroclastic fall deposits 3 explosive events emplacing pyroclastic flow deposits (4<VEI<5) | Yes | - |
| Andronico and Cioni (2002) | Somma-Vesuvio | from Avellino eruption to 79 A.D. | Pyroclastic fall and diluted pyroclastic flow | 2 sub-Plinian to phreato-Plinian eruptions 4 violent strombolian to vulcanian eruptions | Yes | - |
| Todesco et al. (2002) | Somma-Vesuvio | | Pyroclastic flow | | - | Yes |
| Cioni et al. (2003) | Somma-Vesuvio | <18 ka | Pyroclastic fall | 24 explosive events (3<VEI<6) | Yes | Yes |
| Rolandi et al. (2004) | Somma-Vesuvio | 472 A.D. | Pyroclastic fall and pyroclastic flow | 1 | Yes | - |
| Macedonio et al. (2008) | Somma-Vesuvio | | Pyroclastic fall | | - | Yes |
| Lirer et al. (2001b) | Campi Flegrei | <10 ka | Pyroclastic fall and pyroclastic flow | 6 explosive eruptions (3<VEI<4) | Yes | Yes |
| Alberico et al. (2002) | Campi Flegrei | <10 ka | Pyroclastic fall and pyroclastic flow | | - | Yes |
| Orsi et al. (2004) | Campi Flegrei | Post NYT (<15) | Pyroclastic fall and pyroclastic flow | 63 explosive eruptions | Yes | - |
| Rossano et al. (2004) | Campi Flegrei | | Pyroclastic flow | | - | Yes |
| Todesco et al. (2006) | Campi Flegrei | <5 ka | Pyroclastic flow | | - | Yes |
| Costa et al. (2009) | Campi Flegrei | | Pyroclastic fall | | - | Yes |
| Alberico et al. (2008) | Ischia Island | <55 ka | Pyroclastic flow | | - | Yes |

toward the east reached the pre-Apennines. Pyroclastic fall deposits of lower magnitude eruptions almost exclusively blanketed the areas close to the different vents (Di Girolamo et al. 1984; Di Vito et al. 1999) and were emplaced within the Campi Flegrei caldera (Orsi et al. 2004; Costa et al. 2009). The absence of a central vent, posed the question of the "where" the next eruption would occur, for the assessment of the hazard due to the propagation of pyroclastic flows. To this aim, Alberico et al. (2002) drew the hazard maps using the spatial probability of occurrence of a new eruption and the frequency distribution of areas invaded by pyroclastic flows for VEI=3 and 4 eruptions. According to Lirer et al. (2001b), the pyroclastic flows of the last 15 ka remain confined inside the Campi Flegrei caldera. Field data, however, testify to the capability of only very dilute pyroclastic flows to surmount the caldera rim (de Vita et al. 1999; Alberico et al. 2005). This evidence is corroborated by the results of Todesco et al. (2006), who applied a numerical model to define hazard flow variables along different topographic profiles in the southeastern sector of Campi Flegrei by simulating an explosive event from a vent located in the Agnano plain. They infer that for large explosive events (mass eruption rate = $1 \times 10^8$ kg/s) obstacles like the hills bordering the caldera do not protect the city of Napoli but reduce flow velocity and dynamic overpressure; for smaller eruptions (mass eruption rate = $2.5 \times 10^7$ kg/s) the flow is stopped by those topographic barriers.

At Ischia, magnitude and impact of future eruptions will probably be similar to those of the Holocene explosive events that occurred on the island (Brown et al. 2008). Likewise Campi Flegrei, the hazard assessment again implies the knowledge of the site of a possible future eruption and to this end Alberico et al. (2008) assessed the probability of opening a new vent by implementing the methodology reported in Alberico et al. (2002) and simulated VEI=3 and 4 eruptions in order to depict both volcanic hazard and risk maps.

## Multi-source volcanic hazard map

The data reported in the volcanic hazard maps of Somma-Vesuvio, Campi Flegrei (Lirer et al. 2001a; Alberico et al. 2002; Petrosino et al. 2004) and Ischia Island (Alberico et al. 2008), were suitably processed to be merged into a single map. We opted to encompass the main hazards posed by all the explosive events that occurred at the three sources in the last 10 ka rather then choose a size for the future explosive event of which the volcanic hazard was being assessed. A new multi-source hazard map was developed that shows the spatial trend and the extent of the different hazard zones at the regional scale and that allows to forecast the areas exposed to volcanic hazard both from Campi Flegrei and Somma-Vesuvio (Fig. 1). Table 3

**Table 2** Fundamentals and main parameters of the papers containing simulations of explosive eruptions

| Paper | Source | Vent location | Kind of simulated event | Model | Number of simulated events | Maps produced |
|---|---|---|---|---|---|---|
| Barberi et al. (1990) | Somma-Vesuvio | Central (41°N 14°E) | Sub-Plinian eruption emplacing pyroclastic fall | Physical advection-diffusion 3D model of Armienti et al. (1988) based on a continuity equation for the mass concentration considering wind field, atmospheric diffusion, and gravity settling | 3,125 simulations with fixed input parameters and different winds sampled between 1962–1976 at Aeronautica Militare meteorological station of Brindis. | Hazard map |
| Todesco et al. (2002) | Somma-Vesuvio | Central (41°N 14°E) | 1631 eruption pyroclastic flow | Numerical model based on some system parameters describing flow evolution (mass flow-rate per unit, angle of propagation of the flow, topographic profile, duration of the flow feeding, and initial magma properties) | 10 simulations performed by varying the different input parameters | |
| Cioni et al. (2003) | Somma-Vesuvio | Central (41°N 14°E) | Sub-Plinian eruption emplacing pyroclastic fall | Physical advection-diffusion 3D model of Armienti et al. (1988) simplified in 2D | 160,000 simulations performed by varying the different input parameters, with 3,125 different wind fields sampled between 1962–1976 at Aeronautica Militare meteorological station of Brindisi | Hazard map |
| Macedonio et al. (2008) | Somma-Vesuvio | Central (41°N 14°E) | Plinian, Sub-Plinian and violent strombolian eruption emplacing pyroclastic fall | Fallout deposits for the first two scenarios modeled using HAZMAP, a model based on a semi-analytical solution of the 2D advection–diffusion–sedimentation equation. Violent strombolian event is modeled by FALL3D, a numerical model based on the solution of the full 3D advection–diffusion–sedimentation equation | For HAZMAP 13149 simulations with different winds extracted from NCEP/NCAR global mesh nearest to Naples (40°N, 15°E) daily in the 1968–2003 time span. For FALL3D 73 simulations using an "average" meteorological year obtained by the 36-year average daily winds extracted from NCEP/NCAR global mesh nearest to Naples (40°N, 15°E) in the 1968-2003 time span | Hazard map |
| Alberico et al. (2002) | Campi Flegrei | The whole of Campi Flegrei area divided into square cells. Vents centered in square cells 1 km side for VEI=3 events (Monte Nuovo type eruptions). Vents centered in square cells 2 km side for VEI=4 events (Averno type eruptions) | VEI=3 and 4 eruptions emplacing pyroclastic flows | Energy line model (Malin and Sheridan 1982) used to define the frequency of invasion by pyroclastic flows joined to the evaluation of probability of vent opening | 124 simulations for VEI=3 eruptions (Heim coefficient=0.1, column collapse height 100 m+vent topographic height) and 37 simulations for VEI=4 eruptions (Heim coefficient =0.1, column collapse height 300 m+vent topographic height) | Hazard and risk maps |
| Rossano et al. (2004) | Campi Flegrei | 14 vents located within the innermost caldera area | Explosive event emplacing pyroclastic flows. Maximum runout distance ranging between >80 km and 0.2 km | Numerical model of a mass-independent gravity driven pyroclastic current which stops for en masse freezing | 16,800 simulations performed by varying the different input parameters (initial velocity, flow thickness, flow yield strength, flow density, flow viscosity) | Hazard maps |
| Todesco et al. (2006) | Campi Flegrei | Agnano plain | Explosive event emplacing pyroclastic flows. Large events =$1.8 \times 10^8$ - $1 \times 10^8$ kg/s mass eruption rate. Small events =$2.5 \times 10^7$ kg/s mass eruption rate | Numerical model based on some system parameters describing flow evolution (mass flow-rate per unit angle of propagation of the flow, topographic profile, | Performed by varying the different input parameters | - |

**Table 2** (continued)

| Paper | Source | Vent location | Kind of simulated event | Model | Number of simulated events | Maps produced |
|---|---|---|---|---|---|---|
| | | | | duration of the flow feeding, and initial magma properties) | | |
| Costa et al. (2009) | Campi Flegrei | Averno-Monte Nuovo area Agnano-San Vito area | High, medium, and low-magnitude explosive eruptions emplacing pyroclastic fall | HAZMAP computational model (Macedonio et al. 2005), based on a semi-analytical solution of the 2D advection–diffusion–sedimentation equation for volcanic tephra. The input parameters are total erupted mass, eruption column height, and bulk and components distribution | More than 13,000 simulations with different winds sampled by NOAA global mesh nearest to Naples (40°N, 15°E) daily in the 1968–2003 time span | Hazard map |
| Alberico et al. (2008) | Ischia Island | The whole of Ischia Island area divided into square cells. Vents centered in square cells 1 km side both for VEI=3 and 4 events | VEI=3 and 4 eruptions emplacing pyroclastic flows | Energy line model (Malin and Sheridan 1982) used to define the frequency of invasion by pyroclastic flows joined to the evaluation of probability of vent opening | 56 simulations for VEI=3 eruptions (Heim coefficient=0.1, column collapse height 100 m+vent topographic height) and 56 simulations for VEI=4 eruptions (Heim coefficient =0.1, column collapse height 300 m+vent topographic height) | Hazard and risk maps |

summarizes the input data used as a basis of the multi-source hazard map.

## Methodology

The methodology adopted to draw the multi-source hazard map was based on the potentiality of spatial analysis supplied by Geographic Information System (GIS) framework. Many papers published over the last decade prove that GIS software is useful in assessing volcanic hazard (Araña et al. 2000; Pareschi et al. 2000; Gómez-Fernández 2000; Behncke et al. 2006; Felpeto et al. 2007; Toyos et al. 2007; Widiwijayanti et al. 2008) and is a basic tool for practical decision-making in territorial planning and civil protection (Petrosino et al. 2004; Renschler 2005).

The single methodological phases were summarized into flow charts in order to facilitate the reader in following the procedure (Fig. 2a–e).

The first step was the assessment of vent opening probability at Ischia and Campi Flegrei. This value describes the different spatial probabilities of future eruptive event sources for the different points of the volcanic fields. It was quantified by parceling the territory into square cells and applying the spatial analysis to the potential indicators (geo-volcanological, geophysical, and geo-chemical) of a renewal of volcanic activity (Scandone and D'Andrea 1994). The flowchart in Fig. 2a reports a summary of the procedure followed for vent opening probability assessment.

In a second phase, we homogenized the results of our previous research dealing with pyroclastic flow hazard at the three sources. The “energy cone” model (Malin and Sheridan 1982), which assumes column collapse heights of 300 m for eruptions of VEI=4, with Heim coefficient equal to 0.1, was used to perform 37 simulations for Campi Flegrei and 55 for Ischia Island. The simulations were centered in all the square cells previously used to quantify vent opening probability. The overlay of the energy cone to the digital elevation model made it possible to automatically detect the invaded areas for each hypothesized vent. Through the intersection of these areas, we defined the different spatial probabilities of invasion by pyroclastic flow for each point of the territory. The flowchart in Fig. 2b reports the procedure used to assess volcanic hazard related to pyroclastic flows at Campi Flegrei and Ischia Island.

For Somma-Vesuvio, we intersected the areas overrun by the pyroclastic flows of the three main eruptions of the last 10 ka (Avellino, 79 A.D., 472 A.D.). A dynamic overpressure ranging between 1 and 5 kPa was calculated for the pyroclastic flow deposits of 79 A.D. eruption, outcropping in the Terzigno area (Fraldi et al. 2002), about 8 km away from the vent. These values signify a high destructive power on both ancient Roman buildings and on present

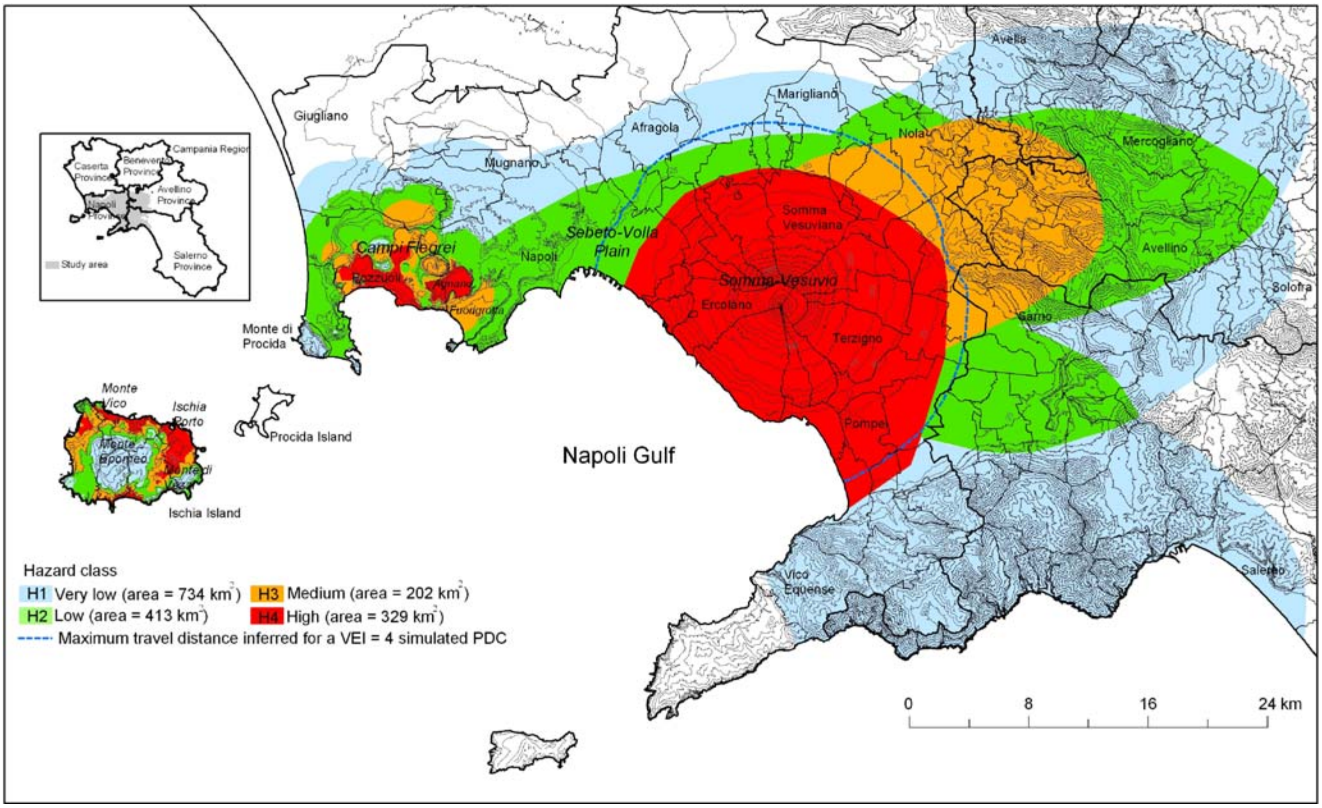


**Fig. 1** Multi-source volcanic hazard map of the Campania Region

**Table 3** Input data used as a basis for drawing the multi-source hazard map

| Source | Vent location | Kinds of products | Field data | Simulated events |
|---|---|---|---|---|
| Somma-Vesuvio | Central (41°N 14°E) | Pyroclastic fall | Isopach maps of 10 explosive events (3<VEI<5) of the last 10 ka | |
| Somma-Vesuvio | Central (41°N 14°E) | Pyroclastic flow | Field boundary of Avellino, 79 A.D. and 472 A.D. pyroclastic flow deposits | |
| Somma-Vesuvio | Central (41°N 14°E) | Pyroclastic flow | | Energy line model (Malin and Sheridan 1982). One simulation for a VEI=4 event. (Heim coefficient = 0.1, column collapse height 300 m+vent topographic height). |
| Campi Flegrei | Agnano Plain | Pyroclastic fall | Isopach maps of the Pomici Principali (ca 10 ka) and Agnano Monte Spina eruptions (ca 4.1 ka) | |
| Campi Flegrei | Vents centered in square cells 2 km side parceling the whole of Campi Flegrei area | Pyroclastic flow | | Energy line model (Malin and Sheridan 1982) joined to the evaluation of probability of vent opening; 37 simulations for VEI=4 eruptions (Heim coefficient = 0.1, column collapse height 300 m+vent topographic height) centered in each cell |
| Ischia Island | Vents centered in square cells 1 km side parceling the whole of Ischia area | Pyroclastic flow | | Energy line model (Malin and Sheridan 1982) joined to the evaluation of probability of vent opening; 56 simulations for VEI=4 eruptions (Heim coefficient = 0.1, column collapse height 300 m+vent topographic height) centered in each cell |

building typologies of the vesuvian area (Nunziante et al. 2003; Zuccaro et al. 2008). Furthermore, a VEI=4 eruption was simulated using the methodology and the input parameters reported in Alberico et al. (2002) in order to make the data comparable for the three sources. A circular hazardous area (Fig. 1) is obtained, slightly larger than that deduced by field survey of outcropping pyroclastic flows deposits. The flowchart in Fig. 2c reports the steps followed to assess pyroclastic flows hazard at Somma-Vesuvio.

Pyroclastic fall hazard assessment at Somma-Vesuvio was based on the isopach maps reported in Lirer et al. (2001a) for the explosive events of the last 10 ka. Different-sized loads of pyroclastic fall deposits have been taken into account to define (for each eruption) the area encompassed by the maximum load sustainable by roofs, stated by the Civil Defence Department at 300 kg/m$^2$ (Dipartimento di Protezione Civile 1995). The intersection of these areas gives a “frequency map”, where single points record how many times the maximum sustainable loading was exceeded in the past 10 ka.

At Campi Flegrei, a methodology similar to Somma-Vesuvio was applied for pyroclastic fall deposits, taking into account the distribution of the products of the two sub-Plinian eruptions of the last 10 ka: Pomici Principali (10.3 ka, Alessio et al. 1973) and Monte Spina (4.1 ka, de Vita et al. 1999). The flowchart in Fig. 2c shows the procedure we followed aiming at pyroclastic fall hazard assessment at Campi Flegrei and Somma-Vesuvio.

The ranking of frequency values allowed us to define four hazard classes for both pyroclastic flows and pyroclastic fall emplacing events at the single source. In Table 4 the labels $H_h$, $H_m$, $H_l$, $H_{vl}$ (where the pedices stand for high, medium, low, and very low), reflect the recurrence of invasion by pyroclastic flows at a single point reclassified according to the *natural break method*, which identifies groups and patterns of data in a set by defining the separation points among the frequency values and minimizing the variance in each class (Jenks and Caspall 1971). For example, the value $H_h$=4 corresponds to the maximum frequency value of 30 for Ischia and 15 for Campi Flegrei, while the number $H_{vl}$=1 corresponds to the minimum frequency value of 2 for Ischia and 1 for Campi Flegrei. For pyroclastic falls, the labels, $H_h$, $H_m$, $H_l$, $H_{vl}$ represent the raw maximum recurrence of products exceeding the overloading threshold.

The final purpose of the procedure was to record (for each point of the studied area) the hazard connected to a possible future event at any of the three sources. To this aim we applied the concept of “weight”, i.e., the frequency of the events normalized according to the maximum frequency registered over the whole multi-source area for the single emplacement mechanism. The weights $w_1$=0.125 and $w_4$=1 were assigned to the areas characterized by lowest and maximum frequency, respectively. Table 4 reports the weight values assigned to the different hazard classes.

**Fig. 2 a–e** Flow chart reporting the procedure for hazard and risk ▶ assessment. **a** Procedure used to assess the vent opening probability at Campi Flegrei and Ischia Island (full details are reported in Alberico et al. 2008). **b** Procedure used to assess the pyroclastic flow hazard at Campi Flegrei and Ischia Island (full details are reported in Alberico et al. 2002, 2008). **c** Procedure used to assess the pyroclastic flow hazard at Somma-Vesuvio and pyroclastic fall hazard at Somma-Vesuvio and Campi Flegrei (full details are reported in Lirer et al. 2001a and Petrosino et al. 2004). **d** Procedure used to draw the multi-source explosive volcanic hazard map for the Campania region. **e** Procedure used to draw the multi-source volcanic risk map for the Campania Region. The input data and the results are reported in *rectangular boxes*, whereas the *elliptical boxes* enclose the map algebra operators and the algorithms applied by using the software ArcGis rel. 9.1

The intersection of hazard areas of the three sources and the sum of relative weights (ranging from $W_1$=0.125 to $W_4$=2) reclassified with the *natural break* method, produced four hazard classes depicted in the multi-source volcanic hazard map of Campania region for tephra and pyroclastic flows (Fig. 2e). Campi Flegrei pyroclastic falls were taken into account only outside of the Campi Flegrei caldera, since their contribution to hazard within the caldera would have masked the effect of topographic obstacles on possible emplacement of pyroclastic flows in the Agnano-Fuorigrotta area.

## Results

Notwithstanding the difficulties found in merging the various hazards posed by the single sources, the multi-source hazard map well depicts the hazard degree of the whole study area. At Somma-Vesuvio all the eruptions emplacing pyroclastic falls in the last 10 ka, strombolian to Plinian in size, were taken into account because the reliability of a hazard map depends on the detail of knowledge of the areas affected by previous events. For pyroclastic flows, we used the emplacement areas of the products of highest VEI events of the same time span together with a VEI=4 simulated event. The resulting circular high hazard area guarantees that the pyroclastic flows of a possible future event will be emplaced within this area. No relationship with the present topography has been investigated, since it would have required a different approach on a much more detailed scale. For Campi Flegrei and Ischia Island, several simulations of pyroclastic flows were necessary to take into account both probability of new vent opening and recurrence of invasion. Furthermore, at these sources, only the maximum size fall emplacing events were considered, because their products were emplaced in wide areas of the Campania Region, whereas the low size eruption fall products mainly blanketed the areas close to the vent.

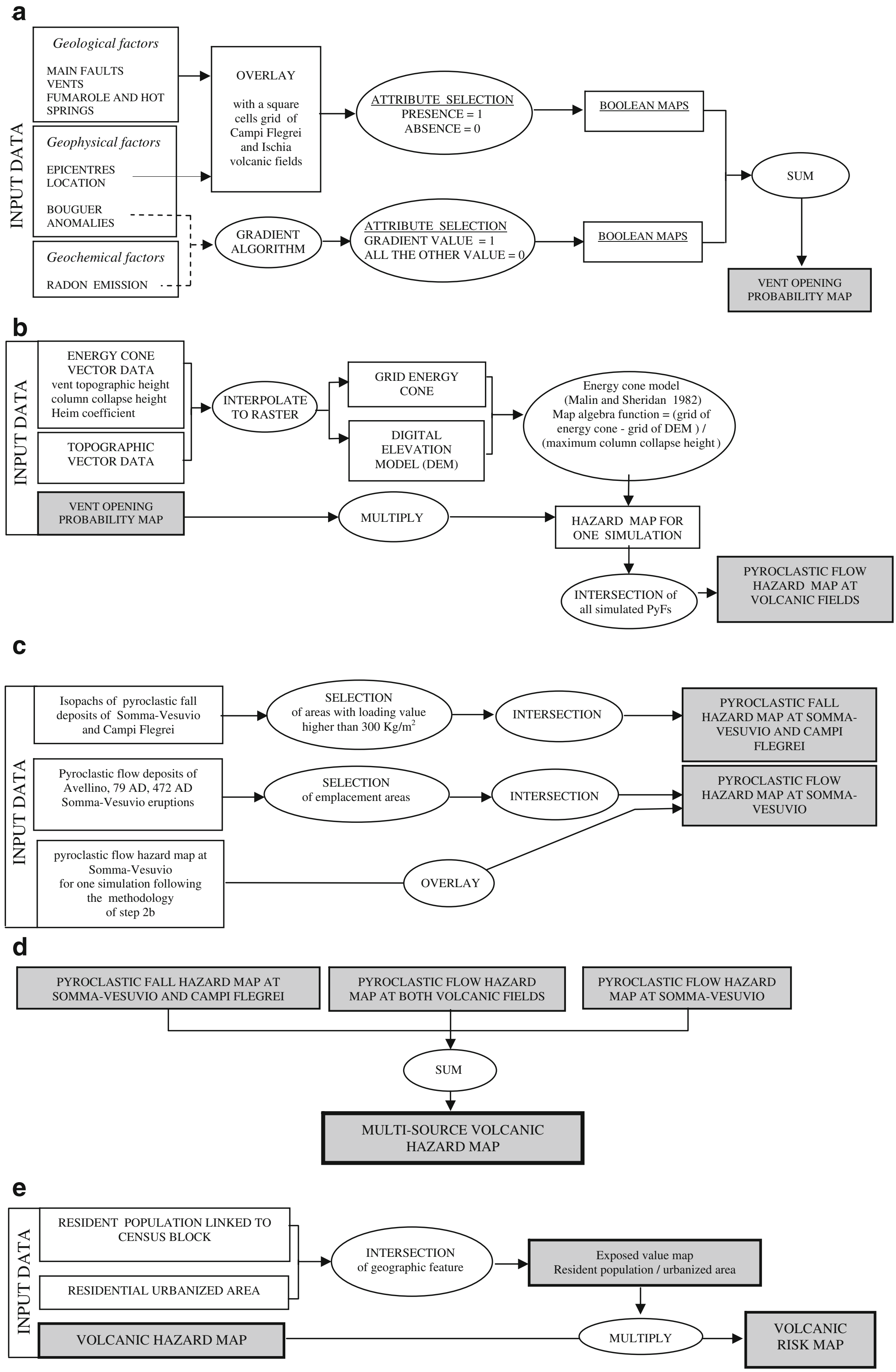
a
INPUT DATA
Geological factors
MAIN FAULTS
VENTS
FUMAROLE AND HOT SPRINGS
Geophysical factors
EPICENTRES LOCATION
BOUGUER ANOMALIES
Geochemical factors
RADON EMISSION
OVERLAY
with a square cells grid of Campi Flegrei and Ischia volcanic fields
ATTRIBUTE SELECTION
PRESENCE = 1
ABSENCE = 0
BOOLEAN MAPS
GRADIENT ALGORITHM
ATTRIBUTE SELECTION
GRADIENT VALUE = 1
ALL THE OTHER VALUE = 0
BOOLEAN MAPS
SUM
VENT OPENING PROBABILITY MAP
b
INPUT DATA
ENERGY CONE VECTOR DATA
vent topographic height
column collapse height
Heim coefficient
TOPOGRAPHIC VECTOR DATA
VENT OPENING PROBABILITY MAP
INTERPOLATE TO RASTER
GRID ENERGY CONE
DIGITAL ELEVATION MODEL (DEM)
Energy cone model (Malin and Sheridan 1982) Map algebra function = (grid of energy cone - grid of DEM ) / (maximum column collapse height )
MULTIPLY
HAZARD MAP FOR ONE SIMULATION
INTERSECTION of all simulated PyFs
PYROCLASTIC FLOW HAZARD MAP AT VOLCANIC FIELDS
c
INPUT DATA
Isopachs of pyroclastic fall deposits of Somma-Vesuvio and Campi Flegrei
SELECTION of areas with loading value higher than 300 Kg/m2
INTERSECTION
PYROCLASTIC FALL HAZARD MAP AT SOMMA-VESUVIO AND CAMPI FLEGREI
Pyroclastic flow deposits of Avellino, 79 AD, 472 AD Somma-Vesuvio eruptions
SELECTION of emplacement areas
INTERSECTION
PYROCLASTIC FLOW HAZARD MAP AT SOMMA-VESUVIO
pyroclastic flow hazard map at Somma-Vesuvio for one simulation following the methodology of step 2b
OVERLAY
d
PYROCLASTIC FALL HAZARD MAP AT SOMMA-VESUVIO AND CAMPI FLEGREI
PYROCLASTIC FLOW HAZARD MAP AT BOTH VOLCANIC FIELDS
PYROCLASTIC FLOW HAZARD MAP AT SOMMA-VESUVIO
SUM
MULTI-SOURCE VOLCANIC HAZARD MAP
e
INPUT DATA
RESIDENT POPULATION LINKED TO CENSUS BLOCK
RESIDENTIAL URBANIZED AREA
VOLCANIC HAZARD MAP
INTERSECTION of geographic feature
Exposed value map
Resident population / urbanized area
MULTIPLY
VOLCANIC RISK MAP

**Table 4** Weight value assigned to define the hazard classes for the areas of Campania region reached by pyroclastic fall and flow deposits of Somma-Vesuvio, Campi Flegrei, and Ischia Island volcanic sources. The *star* points out the weight values taken into account only outside the Campi Flegrei caldera (see text for full details)

| | Pyroclastic flows | | | | | | | | Pyroclastic falls | | | | | | | | Sum | | | |
|---|---|---|---|---|---|---|---|---|---|---|---|---|---|---|---|---|---|---|---|---|
| | $H_{vl}$ | $H_l$ | $H_m$ | $H_h$ | $w_1=H_{vl}/H_h$ | $w_2=H_l/H_h$ | $w_3=H_m/H_h$ | $w_4=H_h/H_h$ | $H_{vl}$ | $H_l$ | $H_m$ | $H_h$ | $w_1=H_{vl}/H_h$ | $w_2=H_l/H_h$ | $w_3=H_m/H_h$ | $w_4=H_h/H_h$ | W1 | W2 | W3 | W4 |
| Somma-Vesuvio | - | - | - | 4 | - | - | - | 1 | 1 | 2 | 3 | 8 | 0.125 | 0.250 | 0.375 | 1 | 0.125 | 0.250 | 0.375 | 2 |
| Campi Flegrei | 1 | 2 | 3 | 4 | 0.250 | 0.500 | 0.750 | 1 | 1 | 2 | - | - | 0.125* | 0.250* | - | - | 0.250 | 0.500 | 0.750 | 1 |
| Ischia Island | 1 | 2 | 3 | 4 | 0.250 | 0.500 | 0.750 | 1 | - | - | - | - | - | - | - | - | 0.250 | 0.500 | 0.750 | 1 |

Four hazard areas with different features were identified in the multi-source volcanic hazard map (Fig. 1). Table 5 reports the spatial extent of the hazard classes for the provinces of the entire investigated area (Napoli, Avellino, Benevento, Salerno):

1. H4 (high hazard): this class corresponds to the perivolcanic area of Somma-Vesuvio, where the highest damage to structures caused by both the impact of pyroclastic flows and the loads exerted on the roofs by pyroclastic falls is expected. This class, also located in the lowland of Campi Flegrei and at Ischia Island, encompasses the whole graben of Ischia and the coastal plain between Monte Vico and Ischia Porto. These areas display high spatial probability of being reached by pyroclastic flows and high damage to structures caused by their impact is expected.
2. H3 (medium hazard): this class is located northeast of Somma-Vesuvio and bounds the high hazard areas at Campi Flegrei and Ischia Island. At Somma-Vesuvio, the hazard is due to the deposition of pyroclastic fall deposits, even if here their recurrence is lower than in the perivolcanic area. At Campi Flegrei and Ischia Island the spatial frequency of pyroclastic flows in this class is lower than in the H4 owing to its average higher altitude; damages caused by pyroclastic flows are expected.
3. H2 (low hazard): this class encircles the Somma-Vesuvio volcano and encompasses the city of Napoli, expanding towards the west in the external area of Campi Flegrei caldera. At Ischia Island, it corresponds to the areas bounding the H3, the average altitude of which is higher than 200 m. These areas display a low recurrence of pyroclastic flows and fall products.
4. H1 (very low hazard): at Somma-Vesuvio, this class surrounds the low hazard area and also encompasses the main part of Penisola Sorrentina; at Campi Flegrei it corresponds to the peripheral zones just outside the Campi Flegrei caldera, at Ischia Island to the Monte Epomeo and Monte di Vezzi areas. This class is characterized by the lowest spatial probability to be hit by the products of explosive activity recorded in the study area.

In this map the blue dotted line shows the maximum travel distance inferred for a VEI=4 simulated pyroclastic flow at Somma-Vesuvio. It indicates that, according to our simulation, the eastern part of the city of Napoli can be reached by pyroclastic flows, as it has already occurred in the past. Alberico et al. (2005), in fact, in many boreholes in the eastern zone of the city found buried pyroclastic flow deposits of the Ottaviano eruption (8 ka, Rolandi et al. 1993a), decreasing in thickness towards the southwest. Moreover, Mastrolorenzo et al. (2006) identified a 3- to

**Table 5** Spatial extent of hazard classes of the four provinces of Campania Region exposed to explosive activity of Somma-Vesuvio, Campi Flegrei, and Ischia Island

| Province | Hazard class | Area ($km^2$) | Area hazard class/total area of hazard class for each province | Province | Hazard class | Area ($km^2$) | Area hazard class/total area of hazard class for each province |
|---|---|---|---|---|---|---|---|
| Napoli | H1 | 277.33 | 30.73 | Avellino | H1 | 180.27 | 48.99 |
| | H2 | 192.63 | 21.35 | | H2 | 120.29 | 32.69 |
| | H3 | 117.48 | 13.02 | | H3 | 67.44 | 18.33 |
| | H4 | 314.98 | 34.90 | | H4 | - | |
| Sum | | 902.42 | | Sum | | 368.01 | |
| Salerno | H1 | 272.83 | 67.33 | Benevento | H1 | 3.24 | 100 |
| | H2 | 100.53 | 24.81 | | H2 | - | |
| | H3 | 17.38 | 4.29 | | H3 | - | |
| | H4 | 14.48 | 3.57 | | H4 | - | |
| Sum | | 405.22 | | | | | |

0.5-m-thick pyroclastic surge deposit that was emplaced by the passage of the last and most powerful Avellino surge cloud sequence, as previously pointed out by Santacroce (1987) and Cioni et al. (1999).

The analysis of the multi-source volcanic hazard map of the Campania Region makes it possible to highlight: (a) the different spatial distribution of the single hazard class at Ischia and Campi Flegrei, (b) the larger extent of the single hazard class at Somma-Vesuvio with respect to Campi Flegrei and Ischia, (c) the presence of large areas exposed to hazard both from Campi Flegrei and Somma-Vesuvio.

The different topography of Campi Flegrei and Ischia Island influenced the distribution of the areas endangered by pyroclastic flows. At Ischia Island, Monte Epomeo (altitude = 787 m a.s.l.) behaved as a main obstacle with respect to the other lower monogenetic volcanoes of the island. This topographic height, located in the center of the island, facilitates the propagation towards the sea of pyroclastic flows sourcing on its slopes, which is further favored by the absence of obstacles that thwart their flows. Monte Epomeo, on the counterpart, represents an obstacle for pyroclastic flows from vents located in the plain. At Campi Flegrei the flow paths were strongly influenced by the position of the vents and by the monogenetic volcanoes scattered inside the Neapolitan Yellow Tuff caldera, behaving as topographic obstacles. This result well resembles the behavior of currents deduced by field data. In fact, According to Lirer et al. (2001b), the pyroclastic flows of the last 15 ka were confined inside the Campi Flegrei caldera, usually thickening in the morphological lowland and thinning toward the slopes that border the intra-calderic plains (Rosi and Sbrana 1987). Moreover, field data indicate that only very dilute pyroclastic flows surmounted the Campi Flegrei caldera rim (200 m average altitude). In particular, the pyroclastic flows of the main phase of the Agnano Monte Spina eruption, channeled along morphological saddles, reached the city of Napoli and overtopped the northeastern slopes of the hills bordering the caldera (de Vita et al. 1999).

In the future, both Somma-Vesuvio and Campi Flegrei explosive products could be emplaced in the large area, surrounding Napoli city, the municipalities located north of Napoli city and at the foot slopes of Somma volcano (Somma-Vesuviana, S. Anastasia etc.).

The plot in Fig. 3a shows the occurrence of the single hazard classes in all the Campania provinces, and the plot

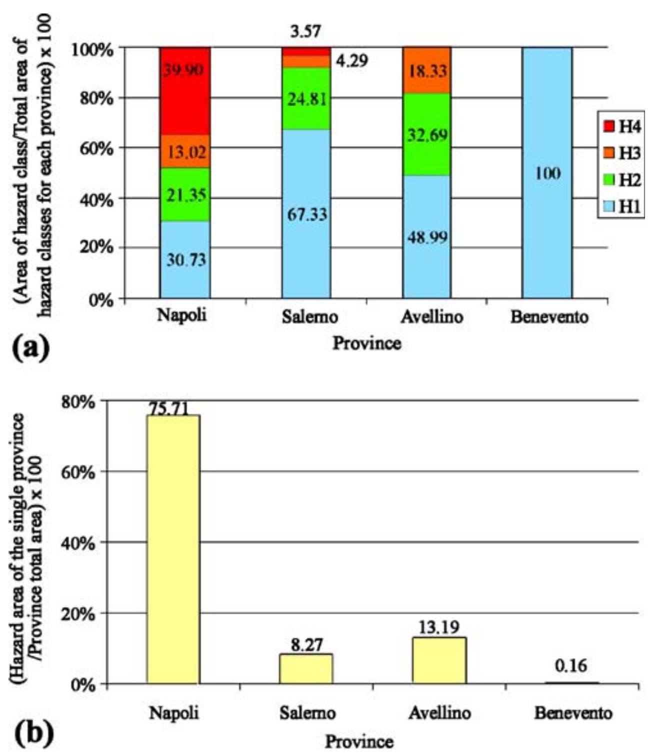


**Fig. 3** Bar plots of the area exposed to the activity of Somma-Vesuvio, Campi Flegrei, and Ischia island. **a** Occurrence of the various hazard classes in the single Campania province. **b** Percentage of the area exposed to hazard in the single Campania province

in Fig. 3b shows the percentage of the area exposed to hazard in each province. Both plots highlight that Napoli province, though the less extended, presents the largest area exposed to hazard and the maximum occurrence of the highest hazard areas.

## Exposure map

### Methodology

In the present paper exposure represents the element at risk in terms of resident population (Alberico et al. 2002, 2008; Dao and Peduzzi 2004; Meloy 2006) and takes into account the real spatial extent of the urban area where people live. In order to obtain an exposure parameter more reliable than the simple population density over municipality area, we drew a dasymetric map (Fig. 4) that depicts quantitative spatial data using boundaries that divide the mapped area into zones of relative homogeneity in order to portray the population density distribution (Eicher and Brewer 2001; Mennis 2003; Chen et al. 2004). The intersection of the resident population for single census block, the smallest geographic unit used for tabulation of housing data (ISTAT 2001), with the occupied residential area (Cartografia Tecnica scale 1:5000 of the Campania Region) allowed us to calculate the population density index. This index (ranging between 0 and 1) is the ratio between the resident population and the extent of urban area attribute value, normalized according to its maximum value over the whole territory.

The Scott formula (1979):

$$k = \frac{\max(X) - \min(X)}{3,5\sigma} n^{1/3}$$

where max(X) and min(X) are the maximum and minimum values of the distribution, respectively; n=number of samples; σ=standard deviation of the distribution, was used to define the classes number ($k$) since the values of the indices of statistical variability and of the Kolmogorov-Smirnov normality test pointed out a normal distribution with a positive skewness (mean>median) and few outliers (kurtosi <3) (Table 6a, b). A statistical analysis was then used to compare the mean error associated to standard deviation, quantile, and natural break classification methods (Table 6c). Finally, we adopted the natural break classification method, since it gave the lowest total error to parcel the whole territory according to the spatial distribution of the population density index.

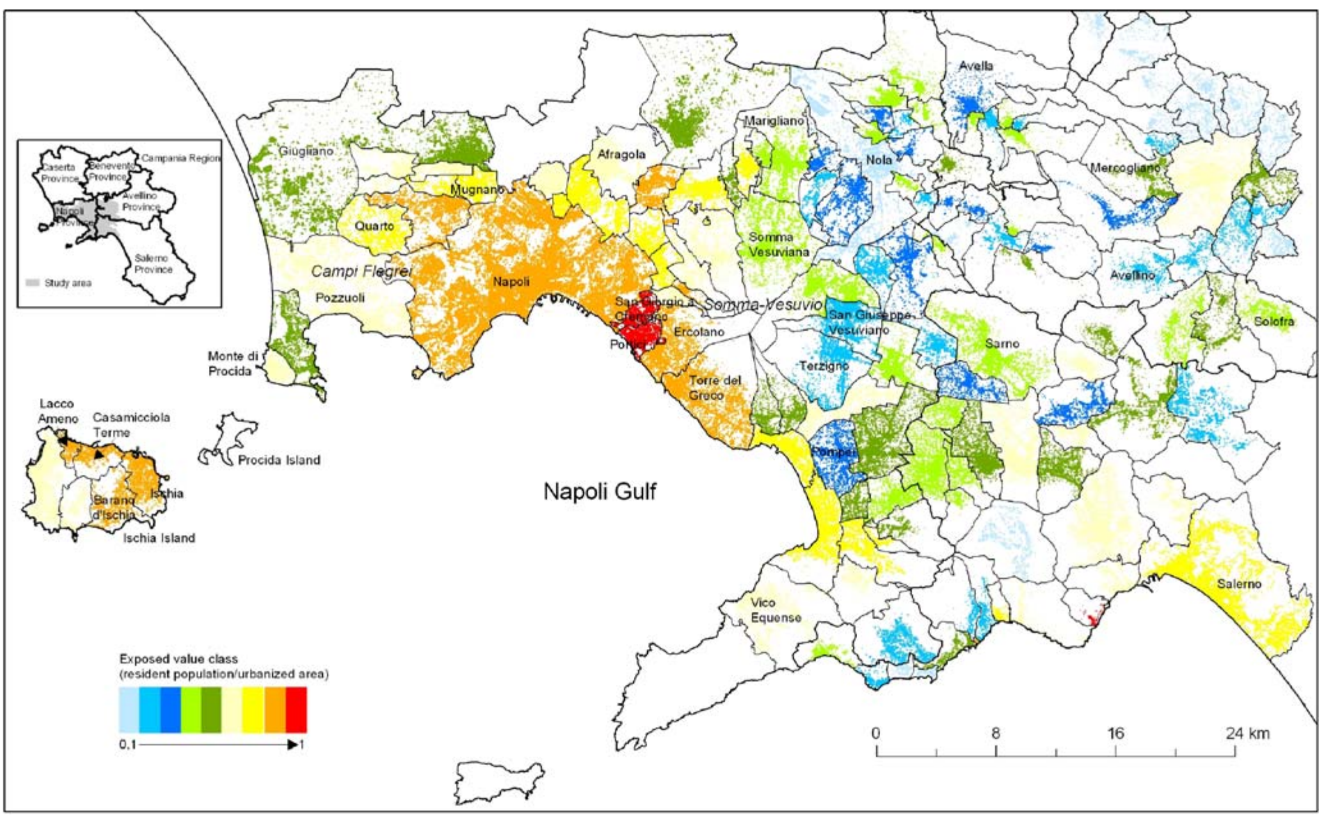


**Fig. 4** Exposure map of single municipalities possibly involved by a future explosive event at any of the three sources. The *red color* indicates the highest exposure while *light blue* indicates a very low exposure

**Table 6** **a**, **b**, **c** Statistical analysis of exposures. **a** Results of the Kolmogorov-Smirnov test. **b** Statistical parameters. **c** Mean error associated with the three distinct classification methods

| **Municipalities n** | 141 |
|---|---|
| **Mean** | 0.36 |
| **Median** | 0.33 |
| **Std. Deviation** | 0.14 |
| **Variance** | 0.019 |
| **Skewness** | 1.32 |
| **Kurtosis** | 2.79 |
| **Minimum** | 0.15 |
| **Maximum** | 1.00 |

**(a)**

| | | **Population density index** |
|---|---|---|
| **Municipalities n** | | 141 |
| **Normal parameters** | Mean | 0.024 |
| | Std. Deviation | 0.009 |
| **Most extreme differences** | Absolute | 0.111 |
| | Positive | 0.111 |
| | Negative | -0.085 |
| **Kolmogorov-Smirnov Z** | | 1.31 |
| **Asymp.Sigma (2-tailed)** | | 0.064 |

**(b)**

| | **Class mean error** | | | | | | | | | **Total error** |
|---|---|---|---|---|---|---|---|---|---|---|
| **Classification method** | 1 | 2 | 3 | 4 | 5 | 6 | 7 | 8 | 9 | |
| Natural Break | 0.118 | 0.159 | 0.106 | 0.273 | 0.211 | 0.284 | 0.319 | 0.336 | 0.261 | 0.015 |
| Standard Deviation | 0.039 | 0.522 | 0.630 | 0.260 | 0.248 | 0.147 | 0.165 | 0.023 | 0.381 | 0.017 |
| Quantile | 0.210 | 0.086 | 0.151 | 0.120 | 0.162 | 0.312 | 0.122 | 0.290 | 1.372 | 0.020 |

**(c)**

## Results

Population density index values close to 1 (high number of resident people in a narrow urban area) generally coincide with a structure typology mainly made up of several stories, typical of S. Giorgio a Cremano and Portici municipalities. Values close to 0 characterize a building typology with residential zones and one and/or two-story buildings (Nola municipality).

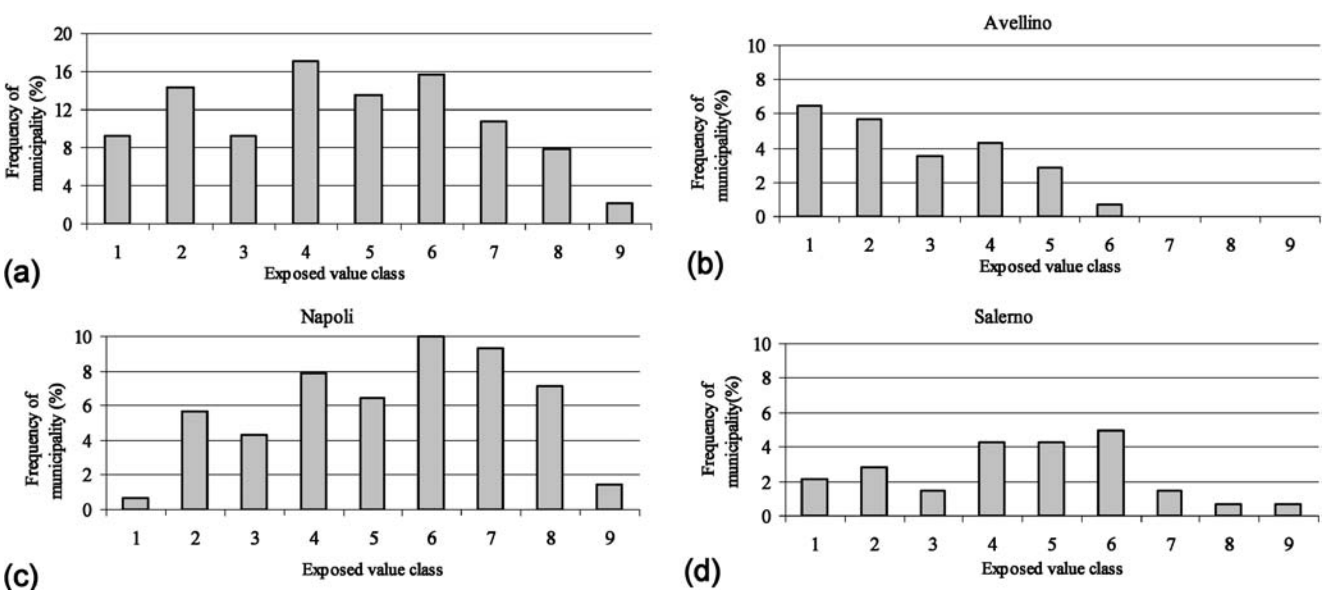


**Fig. 5** Plots of frequency distribution of the exposure classes for **a** all municipalities, **b** Avellino province, **c** Napoli province, and **d** Salerno province

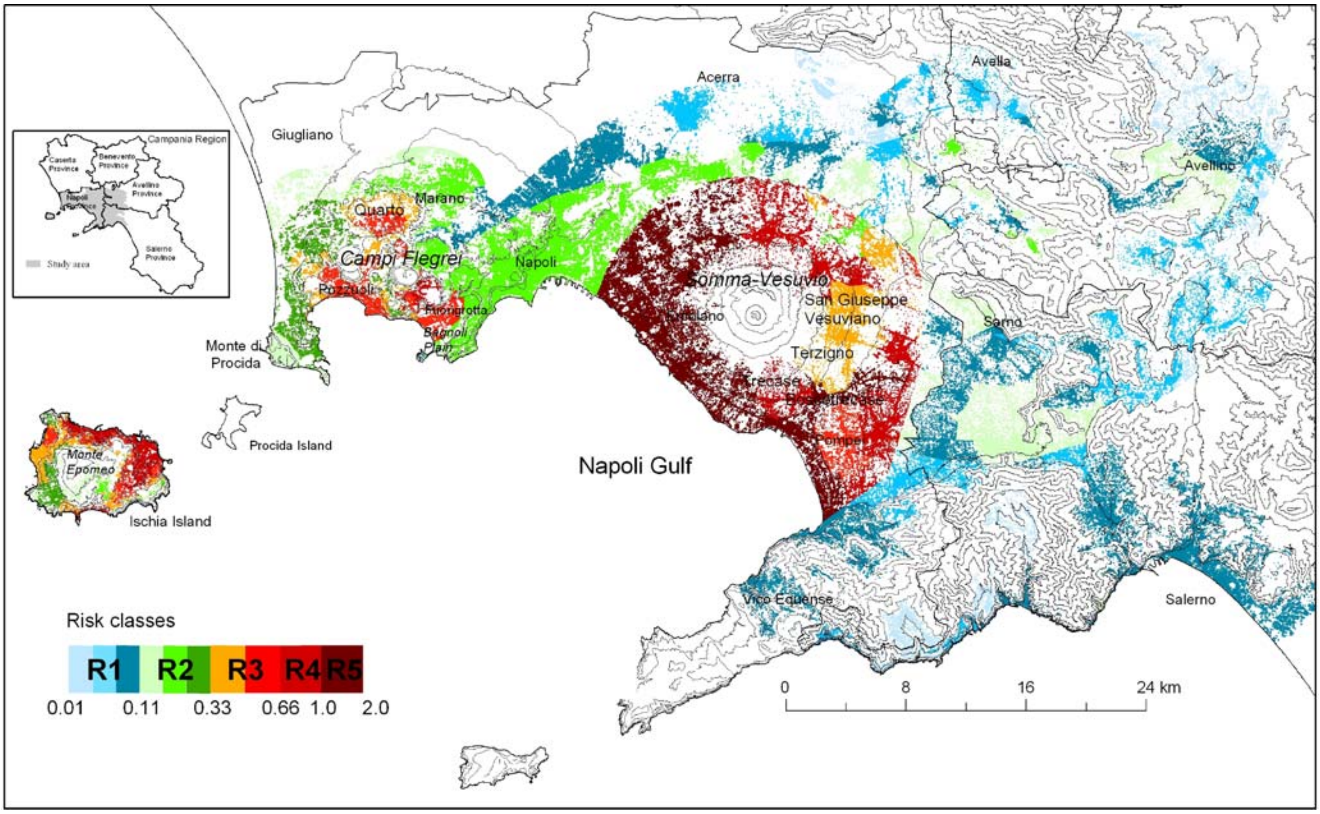


**Fig. 6** Multi-source volcanic risk map of the Campania Region. The entire territory was divided into ten classes. The *red shades* indicate the highest risk areas while the *light blue* indicates very low risk areas

Values ranging between 0 and 1 indicate an intermediate condition.

The frequency distribution of the exposure makes it possible to argue that the number of municipalities falling in each class is quite comparable, except for n.9 class, which concerns only three municipalities (Fig. 5a). On the whole, the municipalities of the Avellino province belong to the low exposure classes (Fig. 5b): those towns, in fact, display large areas devoted to agriculture and the buildings are typically one or two stories detached houses. The municipalities of the Napoli province show high frequencies in the highest exposure classes (Fig. 5c); Salerno behaves as Napoli, even if frequency values are much lower (Fig. 5d), in response to the lower number of municipalities exposed to hazard.

**Table 7** **a**, **b** Statistical analysis of risk. **a** Results of Kolmogorov-Smirnov test. **b** Statistical parameters

**(a)**

| | |
|---|---|
| **Polygons n** | 245 |
| **Mean** | 0.31 |
| **Median** | 0.12 |
| **Std. Deviation** | 0.43 |
| **Variance** | 0.19 |
| **Skewness** | 2.16 |
| **Kurtosis** | 3.99 |
| **Minimum** | 0.01 |
| **Maximum** | 2.00 |

**(b)**

| | | **Risk value** |
|---|---|---|
| **Polygons n** | | 245 |
| **Normal parameters** | Mean | 0.31 |
| | Std. Deviation | 0.43 |
| **Most extreme differences** | Absolute | 0.31 |
| | Positive | 0.31 |
| | Negative | -0.24 |
| **Kolmogorov-Smirnov Z** | | 4.97 |
| **Asymp.Sigma (2-tailed)** | | 0.00 |

## Risk map

### Methodology

When drawing the risk map, the vulnerability in the UNDRO (1979) formula was posed = 1, due to the unavailability of a global vulnerability assessment for the entire study area. Because of this, the risk map is the graphic result of the intersection of hazard and exposure maps (Fig. 6). The risk value associated with these new polygons displayed a non-normal distribution, a positive skewness and σ>3 kurtosis, testifying to the presence of several samples in the tails of the

**Table 8** Double-entry matrix showing the results of the multiplication of hazard values by exposure using different colors for the five risk zones

| Exposure class | Hazard value class 0.125 | 0.250 | 0.375 | 0.500 | 0.75 | 1.000 | 1.125 | 1.250 | 2.000 |
|---|---|---|---|---|---|---|---|---|---|
| 0.11 | 0.014 | 0.028 | 0.041 | 0.055 | 0.083 | 0.110 | 0.124 | 0.138 | 0.220 |
| 0.22 | 0.028 | 0.055 | 0.083 | 0.110 | 0.165 | 0.220 | 0.248 | 0.275 | 0.440 |
| 0.33 | 0.041 | 0.083 | 0.124 | 0.165 | 0.248 | 0.330 | 0.371 | 0.413 | 0.660 |
| 0.44 | 0.055 | 0.110 | 0.165 | 0.220 | 0.330 | 0.440 | 0.495 | 0.550 | 0.880 |
| 0.55 | 0.069 | 0.138 | 0.206 | 0.275 | 0.413 | 0.550 | 0.619 | 0.688 | 1.100 |
| 0.66 | 0.083 | 0.165 | 0.248 | 0.330 | 0.495 | 0.660 | 0.743 | 0.825 | 1.320 |
| 0.77 | 0.096 | 0.193 | 0.289 | 0.385 | 0.578 | 0.770 | 0.866 | 0.963 | 1.540 |
| 0.88 | 0.110 | 0.220 | 0.330 | 0.440 | 0.660 | 0.880 | 0.990 | 1.100 | 1.760 |
| 1.00 | 0.125 | 0.250 | 0.375 | 0.500 | 0.750 | 1.000 | 1.125 | 1.250 | 2.000 |

distribution (Table 7a, b). As a consequence the Friedman and Diaconis (1981) formula,

$$k = \frac{\max(X) - \min(X)}{2IQR} n^{\frac{1}{3}}$$

where

$$IQR = Q_3 - Q_1 (Q = quartile)$$

was chosen because it is more resistant to the extreme values, and used to define the class number. The graphic representation of the high number of classes defined through this procedure would have reduced the effectiveness with which thematic maps represent general patterns for researchers and decisional makers (Mac Eachren 1982). The human eye, in fact, can identify only seven or eight different shadings (Muller 1979), so an alternative representation was used by dividing the whole of the territory into five zones, with values ranging between 0, 1 (very low risk), and 2 (very high risk). Table 8 is a double-entry matrix reporting the results of the multiplication of hazard values (first row) by exposure (first column), using different colors for the five zones into which the territory was finally divided. In the map of Fig. 6, the first three classes are divided into subclasses, for which different shades of the same color were used to better recognize specific detail in the spatial distribution of risk classes. This further subdivision was forced by the high concentration of data in the first three classes.

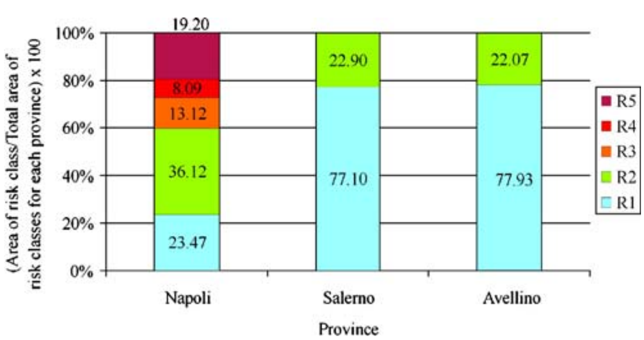


**Fig. 7** Plot of the percentage of the Campania area exposed to volcanic risk in the single province possibly endangered by a future explosive event

## Results

The Avellino and Salerno provinces show low and very low risk values in response to both low exposure and low hazard, only posed by the possible emplacement of Somma-Vesuvio pyroclastic fall deposits. Some 77% of the territory falls in the very low hazard class, and the remaining 23% in the low class (Fig. 7; Table 9).

Napoli province, where all the volcanic sources lie, displays a larger extent of very high and high risk classes; in detail some 60% of territory belongs to low and very low classes, 13% to medium class, and the remaining 27% to high and very high classes.

The municipalities located in the western and southern sectors of Somma-Vesuvio fall in the highest risk class, apart from Trecase and Boscotrecase, which fall in the high risk class as a consequence of the lower population density index, with respect to the neighboring municipalities. The northeastern sector of Somma-Vesuvio displays high-risk values, apart from Terzigno and San Giuseppe Vesuviano municipalities, which show a medium risk. The only low-risk values of the entire perivolcanic territory are shown by two sub-sectors of the Nola municipality, which, on the whole, has a population density index of 0.11 with respect to the 0.66 average value of the area.

In the risk map we notice an abrupt passage from the high-risk to the low-risk class along the main dispersal direction of the fall products of the Somma-Vesuvio (SW–NE). In the volcanic hazard map, on the contrary, a large area of medium hazard is present along the same direction. The contribution of this high hazard area to the risk map goes lost as a consequence of the low population density of the municipalities located in those zones of the Avellino province. In general, the volcanic risk map becomes less

**Table 9** Spatial extent of risk classes of the four provinces of Campania region exposed to explosive activity of Somma-Vesuvio, Campi Flegrei and Ischia island

| Province | Risk class | Area (km$^2$) | (Area risk class/total area of risk class for each province)*100 | Province | Risk class | Area (km$^2$) | (Area risk class/total area of risk class for each province)*100 |
|---|---|---|---|---|---|---|---|
| **Napoli** | R1 | 18,43 | 23,47 | **Avellino** | R1 | 6,27 | 77,93 |
| | R2 | 28,35 | 36,12 | | R2 | 1,78 | 22,07 |
| | R3 | 10,30 | 13,12 | | R3 | - | - |
| | R4 | 6,35 | 8,09 | | R4 | - | - |
| | R5 | 15,08 | 19,20 | | R5 | - | - |
| *Sum* | | *78,50* | | *Sum* | | *8,05* | |
| **Salerno** | R1 | 14,55 | 77,10 | | | | |
| | R2 | 4,32 | 22,91 | | | | |
| | R3 | - | | | | | |
| | R4 | - | - | | | | |
| | R5 | | | | | | |
| *Sum* | | *18,87* | | | | | |

sensitive to hazard classification as far as the medium, low, and very low classes are concerned.

Within the Campi Flegrei caldera, high hazard corresponds to the high-risk areas, mainly because of the high population density index characterizing the lowlands, where also the volcanic hazard is very high. The only exceptions are the Fuorigrotta area and part of the Bagnoli plain, which display medium hazard and high risk, as a consequence of the high population density. The same behavior is displayed by the Quarto municipality.

Finally, at Ischia Island, the correspondence between high hazard and high-risk zones emerges. Some slight differences can be noticed in the narrower spatial extent of the medium and high-hazard classes with respect to the corresponding risk classes, caused by the presence of buildings along the slopes of Monte Epomeo, which signifies a high population density index in a low-hazard area.

The multi-source risk map here presented can also be drawn at a much larger scale and by using different illustration methods for decision-making, monitoring, and evaluation of territorial planning policies in the perivolcanic areas. As an example, Fig. 8 shows the risk map for Ischia Island depicted by superimposing the risk classes of Fig. 6 onto the orthophoto map. This kind of graphic representation was already proposed in Petrosino et al. (2004), who proved that these maps can be very effective both for territorial decision-makers and for endangered populations. In this regard, Haynes et al. (2007) found that communication of spatial hazard information was improved when using aerial photographs rather than traditional plan-view contour maps. Nevertheless, their use is constrained by the drawing limits, since the representation results are only clear when the scale of the map is large enough to make the territorial elements easily distinguishable.

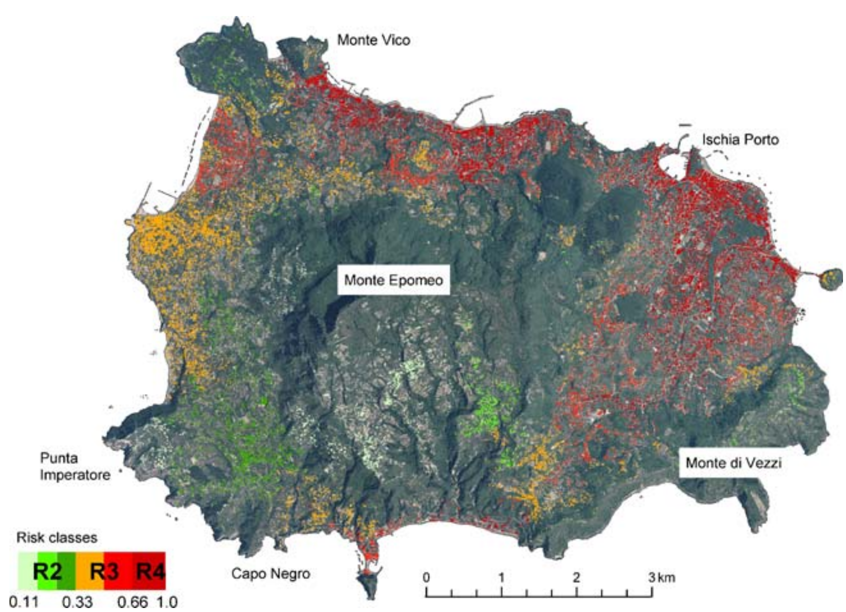


**Fig. 8** Risk classes represented on the ortho-photo map for Ischia Island

## Conclusive remarks

Somma-Vesuvio, Campi Flegrei, and Ischia Island are three volcanic sources located in the Campania Region (southern Italy) currently experiencing a phase of quiescence that will eventually give way to future explosive activity. Although they required some simplification, mainly because of the difficulties in balancing the volcanic hazard posed by a central volcano and two volcanic fields, the multi-source maps produced in the present paper are a very innovative product, since they supply the first global and synoptic view of the areas possibly endangered by pyroclastic fall and flows caused by a future explosive event at any of the three Campania active volcanic sources. These maps are an up-gradable tool because new data can be processed at any time to implement the result and possibly to refine the boundaries of the single hazard zones. As a matter of fact, our present maps do not take into account the syn-eruptive occurrence of lahars and floods, hazardous phenomena strictly related to the past activity of all three volcanoes. The investigation of this hazard was beyond the object of this paper, but our multi-source hazard and risk maps can be combined with flooding hazard data in the future to draw a comprehensive hazard map. They are an essential tool in the communication of volcanic risk among the scientists, local authorities, and the public, and could prove their utility for the long-term and regional scale for mitigation purposes. These maps, in fact, are not particularly appropriate for an on-going volcanic crisis, when very detailed hazard representations as those reported in Petrosino et al. (2004) or Alberico et al. (2006) would certainly fit better, but represent a vital tool for territorial planning in areas exposed to volcanic hazard. Both volcanic hazard and risk maps could be used by local government officials of the Campania Region as a basic tool for decision-making regarding territorial management and future planning throughout an entire region. Too often, in fact, local authorities lack a global vision of a possible impending hazard and territorial development carries on in complete disregard of risk factors. Nevertheless, single subsets of the multi-source maps can also be drawn on a larger scale with different formats and become effective in managing volcanic crises, and establish preparatory, response, and recovery actions related to volcanic risk.

**Acknowledgements** A. Rapolla is gratefully acknowledged for reading an early version of the paper. The authors also wish to gratefully thank the reviewers C. Bonadonna, J. Barclay, and S. J. Cronin for thoughtful and constructive comments on the manuscript. A sincere thank-you goes to associate editor R. Cioni whose suggestions greatly improved the paper and to P. Sclafani for revising the English text.

## References

Alberico I, Lirer L, Petrosino P, Scandone R (2002) A methodology for the evaluation of volcanic risk in Campi Flegrei. J Volcanol Geotherm Res 116:63–78

Alberico I, Petrosino P, Zeni G, D'Andrea F, Lirer L (2005) GEOCITY: a drill-hole database as tool to assess geological hazard in Napoli urban area. Environ Geol 47:751–762

Alberico I, Bruno L, Dal Piaz A, Lirer L, Petrosino P (2006) Urban management to mitigate natural hazard: Urban management in area exposed to natural hazard: an example from Campi Flegrei (southern Italy) SAGEO 2006 International Conference on Spatial Analysis and GEOmatics, Strasbourg, 11–13 September 2006

Alberico I, Lirer L, Petrosino P, Scandone R (2008) Volcanic hazard and risk assessment from pyroclastic flows at Ischia Island (southern Italy). J Volcanol Geotherm Res 171:118–136

Alessio M, Bella F, Improta S, Belluomini G, Cortesi C, Turi F (1973) University of Rome Carbon-14 dates. X Radiocarbon 15:165–178

Andronico D, Cioni R (2002) Contrasting styles of Mount Vesuvius activity in the period between the Avellino and Pompeii Plinian eruptions, and some implications for assessment of future hazards. Bull Volcanol 64:372–391

Araña V, Felpeto A, Astizba M, García A, Ortiza R, Abella R (2000) Zonation of the main volcanic hazards (lava flows and ash fall) in Tenerife, Canary Islands. A proposal for a surveillance network. J Volcanol Geotherm Res 103(1–4):377–391

Arrighi S, Principe C, Rosi M (2001) Violent strombolian and subplinian eruptions at Vesuvius during post-1631 activity. Bull Volcanol 63:126–150

Barberi F, Macedonio G, Pareschi MT, Santacroce R (1990) Mapping the tephra fallout risk: an example from Vesuvius (Italy). Nature 344:142–144

Baxter PJ, Aspinall WP, Neri A, Zuccaro G, Spence RJS, Cioni R, Woo G (2008) Emergency planning and mitigation at Vesuvius: a new evidence-based approach. J Volcanol Geotherm Res 178:454–473

Behncke B, Neri M, Pecora E, Zanon V (2006) The exceptional activity and growth of the Southeast Crater, Mount Etna (Italy), between 1996 and 2001. Bull Volcanol 69:149–173

Brown RJ, Orsi G, De Vita S (2008) New insights into Late Pleistocene explosive volcanic activity and caldera formation on Ischia (southern Italy). Bull Volcanol 70:583–603

Chen K, McAneney J, Blong R, Leigh R, Hunter L, Magill C (2004) Defining area at risk and its effect in catastrophe loss estimation: a dasymetric mapping approach. Appl Geog 24:97–117

Cioni R, Santacroce R, Sbrana A (1999) Pyroclastic deposits as a guide for reconstructing the multi-stage evolution of the Somma-Vesuvius caldera. Bull Volcanol 60:207–222

Cioni R, Longo A, Macedonio G, Santacroce R, Sbrana A, Sulpizio R, Andronico D (2003) Assessing pyroclastic fall hazard through field data and numerical simulation: example from Vesuvius. J Geophys Res 103:2063–2073

Civetta L, D'Antonio M, di Lorenzo S, Di Renzo V, Gasparini P (2004) Thermal and geochemical constraints to the deep magmatic structure of Mount Vesuvius. J Volcanol Geotherm Res 133:1–12

Coburn AW, Spence RJS, Pomonis A (1991) Vulnerability and risk assessment. UNDP Disaster Management Training Program, New York, pp 1–57

Costa A, Dell'Erba F, Di Vito MA, Isaia R, Macedonio G, Orsi G, Pfeiffer T (2009) Tephra fallout hazard assessment at the Campi Flegrei caldera (Italy). Bull Volcanol 71:259–273

D'Antonio M (2005) Calderas and magmatic feeding systems: examples from Campi Flegrei (southern Italy). Acta Vulcanol 17:53–66

D'Antonio M, Civetta L, Orsi G, Pappalardo L, Piochi M, Carandente A, de Vita S, Di Vito MA, Isaia R (1999) The present state of the magmatic system of the Campi Flegrei caldera based on a reconstruction of its behaviour in the past 12 ka. J Volcanol Geotherm Res 91:247–268

Daniele P, Lirer L, Petrosino P, Spinelli N, Peterson R (2009) Applications of the PUFF model to forecasts of volcanic clouds dispersal from Etna and Vesuvio. Comput Geosci 35:1035–1049

Dao H, Peduzzi P (2004) United Nations Environment Programme Global Resource Information Database—Geneva UNEP/DEWA/GRID-Geneva. May 2003, pp 1–31

Deino L, Orsi G, de Vita S, Piochi M (2004) The age of the Neapolitan Yellow Tuff caldera-forming eruption (Campi Flegrei caldera—Italy) assessed by $^{40}Ar/^{39}Ar$ dating method. J Volcanol Geotherm Res 133:157–170

de Vita S, Orsi G, Civetta L, Carandente A, D'Antonio M, Deino A, di Cesare T, Di Vito MA, Fisher RV, Isaia R, Marotta E, Necco A, Ort M, Pappalardo L, Piochi M, Southon J (1999) The Agnano–Monte Spina eruption (4100 years BP) in the restless Campi Flegrei caldera (Italy). J Volcanol Geotherm Res 91:269–301

Di Girolamo P, Ghiara MR, Lirer L, Munno R, Rolandi G, Stanzione D (1984) Vulcanologia e petrologia dei Campi Flegrei. Boll Soc Geol It 103:349–413

Dipartimento della Protezione Civile (1995) Pianificazione nazionale di emergenza dell'area vesuviana. Presidenza del Consiglio dei Ministri Roma 1995, pp 1–55

Di Renzo V, Di Vito MA, Arienzo I, Carandente A, Civetta L, D'Antonio M, Giordano F, Orsi G, Tonarini S (2007) Magmatic history of Somma-Vesuvius on the basis of new geochemical and isotopic data from a deep borehole (Camaldoli della Torre). J Petrol 48:753–784

Di Vito MA, Isaia R, Orsi G, Southon J, de Vita S, D'Antonio M, Pappalardo L, Piochi M (1999) Volcanism and deformation since 12,000 years at the Campi Flegrei caldera (Italy). J Volcanol Geotherm Res 91:221–246

Eicher CL, Brewer CA (2001) Dasymetric mapping and areal interpolation: implementation and evaluation. Cartog Geog Inf Sci 28:125–138

Esposti Ongaro T, Neri A, Todesco M, Macedonio G (2002) Pyroclastic flow hazard assessment at Vesuvio (Italy) by using numerical modelling II. Analysis of flow variables. Bull Volcanol 64:178–191

Felpeto A, Marti J, Ortiz R (2007) Automatic GIS-based system for volcanic hazard assessment. J Volcanol Geotherm Res 166:106–116

Fraldi M, Lirer L, Nunziante L, Petrosino P, Scotellaro S, Cicirelli C (2002) Analysis of AD 79 eruption pyroclastic currents impact and present risk assessment for buildings at Vesuvio. AGU Chapman Conference on Volcanism and the Earth's atmosphere, Santorini, Greece, 17-21 June 2002

Friedman JH, Diaconis P (1981) On the histogram as a density estimator: L2 theory. Z Wahrscheinlichkeitstheor Verw Geb 57:453–476

Gómez-Fernández F (2000) Application of a GIS algorithm to delimit the areas protected against basic lava flow invasion on Tenerife Island. J Volcanol Geotherm Res 103:409–423

Haynes K, Barclay J, Pidgeon N (2007) Volcanic hazard communication using maps: an evaluation of their effectiveness. Bull Volcanol 70:123–138

ISTAT (2001) Census data of the Italian Institute of Statistic. www.istat.it, http://dawinci.istat.it/daWinci

Jenks GF, Caspall FC (1971) Error on choroplethic maps: definition, measurement, reduction. Ann Assoc Am Geog 61:217–244

Lirer L, Munno R, Petrosino P, Vinci A (1993) Tephrostratigraphy of the AD 79 pyroclastic deposits in perivolcanic areas of Mt Vesuvio (Italy). J Volcanol Geotherm Res 58:133–149

Lirer L, Petrosino P, Alberico I, Postiglione I (2001a) Long-term volcanic hazard forecast based on Somma-Vesuvio past eruptive activity. Bull Volcanol 68:145–163

Lirer L, Petrosino P, Alberico I (2001b) Volcanic hazard assessment at volcanic fields: the Campi Flegrei case history. J Volcanol Geotherm Res 101:55–75

Mac Eachren AM (1982) The role of complexity and symbolization method in thematic map effectiveness. Ann Assoc Am Geog 72:495–513

Macedonio G, Costa A, Folch A (2008) Ash fallout scenarios at Vesuvius: numerical simulations and implications for hazard assessment. J Volcanol Geotherm Res 178:366–377

Malin MC, Sheridan MF (1982) Computer-assisted mapping of pyroclastic surges. Science 217:637–640

Mastrolorenzo G, Petrone P, Pappalardo L, Sheridan MF (2006) The Avellino 3780-yr-B.P. catastrophe as a worst-case scenario for a future eruption at Vesuvius. Proc Nat Acad Sci 103:4366–4370

Meloy AF (2006) Arenal-type pyroclastic flows: a probabilistic event tree risk analysis. J Volcanol Geotherm Res 157:121–134

Mennis J (2003) Generating surface models of population using dasymetric mapping. Prof Geog 55:31–42

Muller JC (1979) Perception of continuously shaded maps. Ann Assoc Am Geog 69:240–249

Nunziante L, Fraldi M, Lirer L, Petrosino P, Scotellaro S, Cicirelli C (2003) Analysis of AD 79 eruption pyroclastic currents impact and present risk assessment for buildings at Vesuvio. Bull Volcanol 65:154–176

Orsi G, Di Vito MA, Isaia R (2004) Volcanic hazard assessment at the restless Campi Flegrei caldera. Bull Volcanol 66:514–530

Pareschi MT, Cavarra L, Favalli F, Gianni F, Meriggi A (2000) GIS and volcanic risk management. Nat Haz 21:361–379

Petrosino P, Alberico I, Caiazzo S, Dal Piaz A, Lirer L, Scandone R (2004) Volcanic risk and evolution of the territorial system in the volcanic areas of Campania. Acta Vulcanol 16:163–178

Poli S, Chiesa S, Gillot PY, Gregnanin A, Guichard F (1987) Chemistry versus time in the volcanic complex of Ischia (Gulf of Naples, Italy): evidence of successive magmatic cycles. Contrib Mineral Petrol 95:322–335

Piochi M, Civetta L, Orsi G (1999) Mingling in the magmatic system of Ischia (Italy) in the past 5 ka. Mineral Petrol 66:227–258

Renschler CS (2005) Scales and uncertainties in volcano hazard prediction—optimizing the use of GIS and models. J Volcanol Geotherm Res 139:73–87

Rolandi G, Maraffi S, Petrosino P, Lirer L (1993a) The Ottaviano eruption of Somma-Vesuvio (8,000 Y BP): a magmatic alternating fall and flow forming eruption. J Volcanol Geotherm Res 58:43–65

Rolandi G, Barrella AM, Borrelli A (1993b) The 1631 eruption of Vesuvio. J Volcanol Geotherm Res 58:183–201

Rolandi G, Mastrolorenzo G, Barrella AM, Borrelli A (1993c) The Avellino Plinian eruption of Somma-Vesuvius (3760 y BP): the progressive evolution from magmatic to hydromagnatic style. J Volcanol Geotherm Res 58:67–88

Rolandi G, Petrosino P, Mc Geehin J (1998) The interplinian activity of Somma-Vesuvius in the last 3500 years. J Volcanol Geotherm Res 81:19–52

Rolandi G, Munno R, Postiglione I (2004) The AD 472 eruption of Somma volcano. J Volcanol Geotherm Res 104:67–92

Rosi M, Sbrana A (1987) Phlegrean Fields - CNR, Quaderni de "La Ricerca Scientifica", 114:1–175

Rosi M, Principe C, Vecci R (1993) The 1631 eruption of Vesuvius reconstructed from the review of chronicles and study of deposits. J Volcanol Geotherm Res 58:151–182

Rossano S, Mastrolorenzo G, De Natale G (2004) Numerical simulation of pyroclastic density currents on Campi Flegrei topography: a tool for statistical hazard estimation. J Volcanol Geotherm Res 132:1–14

Santacroce R (1987) Somma-Vesuvius. CNR Quad Ric Sc 114(9):1–251

Santacroce R, Sbrana A, Andronico D, Cioni R, Di Vito M, Marianelli P, Sulpizio R, Zanchetta G, Arrighi S, Benvenuti E, Gurioli L, Leoni FM, Luperini W (2003) Carta geologica del Vesuvio in scala 1:15000. In: Santacroce R, Sbrana A (eds) Cartografia derivata dai rilievi geologici in scala 1:10000 Regione Campania e dai rilievi in scala 1:25000 del Progetto CARG. SELCA, Firenze

Scaillet B, Pichavant M, Cioni R (2008) Upward migration of Vesuvius magma chamber over the past 20,000 years. Nature 455:216–219

Scandone R, D'Andrea M (1994) Il rischio vulcanico. In: Di Donna V, Vallario A (eds) "L'ambiente: Risorse e rischi" Liguori, Napoli, pp 130–150

Scott DW (1979) On optimal and data based histograms. Biometrika 66:605–610

Todesco M, Neri A, Esposti Ongaro T, Papale P, Macedonio G, Santacroce R, Longo A (2002) Pyroclastic flow hazard assessment at Vesuvio (Italy) by using numerical modeling. I Large-scale dynamics. Bull Volcanol 64:155–177

Todesco M, Neri A, Esposti Ongaro T, Papale P, Rosi M (2006) Pyroclastic flow dynamics and hazard in a caldera setting: application to Phlegrean Fields (Italy). Geochem Geophys Geosyst 7:Q11003. doi:101029/2006GC001314

Toyos GP, Cole PD, Felpeto A, Martí J (2007) A GIS-based methodology for hazard mapping of small pyroclastic density currents. Nat Haz 41:99–112

UNDRO (1979) Natural disasters and vulnerability analysis. Report of Expert Group Meeting (9-12 July 1979), UNDRO (United Nations Disaster Relief Coordinator), Geneva

Widiwijayanti C, Voight B, Hidayat D, Schilling SP (2008) Objective rapid delineation of areas at risk from block-and-ash pyroclastic flows and surges. Bull Volcanol. doi:10.1007/s00445-008-0254-6

Zuccaro G, Cacace F, Baxter PJ, Spence R (2008) Impact of explosive scenarios at Vesuvius. J Volcanol Geotherm Res 178:416–453